HHS Public Access

Author manuscript

Nature. Author manuscript; available in PMC 2011 December 23.

Published in final edited form as:

Nature. ; 474(7352): 506–510. doi:10.1038/nature10111.

Antidiabetic actions of a phosphatidylcholine ligand for nuclear receptor LRH-1

Jae Man Lee[1], **Yoon Kwang Lee**[2,3], **Jennifer L. Mamrosh**[2], **Scott A. Busby**[4], **Patrick R. Griffin**[4], **Manish C. Pathak**[5], **Eric A. Ortlund**[5], and **David D. Moore**[1,2,*]

[1]Program in Developmental Biology, Baylor College of Medicine, Houston, TX 77030, USA

[2]Department of Molecular and Cellular Biology, Baylor College of Medicine, Houston, TX 77030, USA

[3]Department of Integrative Medical Sciences, Northeastern Ohio Universities Colleges of Medicine and Pharmacy, Rootstown, OH 44272, USA

[4]The Scripps Research Molecular Screening Center, The Scripps Research Institute, Scripps Florida, Jupiter, FL 33458, USA

[5]Department of Biochemistry, Emory University School of Medicine, Atlanta, GA 30322, USA

Abstract

Nuclear hormone receptors regulate diverse metabolic pathways and the orphan nuclear receptor LRH-1 (NR5A2) regulates bile acid biosynthesis[1,2]. Structural studies have identified phospholipids as potential LRH-1 ligands[3–5], but their functional relevance is unclear. Here we show that an unusual phosphatidylcholine species with two saturated 12 carbon fatty acid acyl side chains (dilauroyl phosphatidylcholine, DLPC) is an LRH-1 agonist ligand *in vitro*. DLPC treatment induces bile acid biosynthetic enzymes in mouse liver, increases bile acid levels, and lowers hepatic triglycerides and serum glucose. DLPC treatment also decreases hepatic steatosis and improves glucose homeostasis in two mouse models of insulin resistance. Both the antidiabetic and lipotropic effects are lost in liver specific *Lrh-1* knockouts. These findings identify an LRH-1 dependent phosphatidylcholine signaling pathway that regulates bile acid metabolism and glucose homeostasis.

*Correspondence and requests for materials should be addressed to D.D.M. (moore@bcm.edu).

Supplementary Information is linked to the online version of the paper at www.nature.com/nature. A figure summarizing the main result of this paper is available in Supplementary Information.

Author Contributions. J.M.L. designed and executed the experiments, interpreted data and cowrote the manuscript. Y.K.L. and J.L.M. helped with experiments. S.A.B. and P.R.G. performed the fluorescence binding experiments, and M.C.P. and E.A.O. performed the mass spectrometry experiment. D.D.M. supervised the design and interpretation of the experiments and cowrote the manuscript.

Author Information The authors declare no competing financial interests.

Statistics

Numbers of mice for each group used in experiments are indicated in the figure legends. Statistical analyses were performed with the 2-tailed Student's t test, and error bars represent means ± s.e.m. P value < 0.05 was considered statistically significant.

Increased fat accumulation in the liver, or steatosis, is tightly correlated with insulin resistance and type 2 diabetes[6]. Modestly elevated bile acid levels decrease steatosis[7]. Loss of the nuclear receptor LRH-1 decreases bile acid levels[1,2], suggesting that an LRH-1 agonist could increase them and improve fatty liver. In screens of a number of different PC and other phospholipid species for effects on human LRH-1 (hLRH-1) transactivation, dilauroyl PC (C12:0/C12:0; DLPC) and diundecanoyl PC (C11:0/C11:0; DUPC) showed strong stimulation (Fig. 1a). Comparable responses were not observed with closely related PCs differing in acyl chain length by only a single methylene group, or with any other C12:0/C12:0 phospholipid species (Supp. Fig. 1a–c).

DLPC and DUPC, but not the bile acid (BA) chenodeoxycholic acid (CDCA) or the more conventional phospholipid dipalmitoyl PC (C16:0/C16:0, DPPC), also activated the synthetic LRH-1 reporter in several other cell lines, including CV-1 and HEK293T cells (data not shown), and specifically increased basal LRH-1 transactivation of the native mouse SHP promoter[8] by approximately 2-fold in HeLa cells (Supp. Fig. 2a). DLPC and DUPC also induced a similar response with the Oct4 promoter, which was dependent on both LRH-1 cotransfection and an intact LRH-1 response element[9] (Supp. Fig. 2a). DLPC and DUPC responsiveness was not altered in mutant LRH-1 derivatives previously shown to inactivate responses to LRH-1 phosphorylation[10] or sumoylation[11], but was strongly decreased by mutations shown to block phospholipid binding[4] (Supp. Fig. 2d).

Mouse and human LRH-1 showed essentially equivalent responses to DLPC and DUPC, and both DLPC and DUPC also activate the close LRH-1 relative SF-1 (Supp. Fig. 2b). The LRH-1 responses were dose dependent (Supp. Fig. 2c). Neither DUPC nor DLPC showed significant activation of any of a number of additional nuclear receptors outside of the NR5A subgroup (Supp. Fig. 2b). In particular, DLPC and DUPC failed to activate PPARα, which was recently reported to be specifically bound and activated by 1-palmitoyl-2-oleoyl (C16:0/C18:1) PC[12], and C16:0/C18:1 PC failed to affect LRH-1 transactivation (Supp. Fig. 1a). DLPC rapidly induced expression of the LRH-1 target Cyp8B1 in the C3A derivative of HepG2 cells (Supp. Fig. 3a). This response, as well as CDCA repression of Cyp8B1 expression and transactivation of a synthetic LRH-1 reporter plasmid was specifically compromised in cells transfected with LRH-1 siRNA (Supp. Fig. 3b, c).

We used the mammalian 2-hybrid assay and a simple GST pulldown approach to initially test the predicted function of DLPC and DUPC as LRH-1 agonist ligands. In the mammalian 2-hybrid analysis, interaction of a VP16-hLRH-1 ligand binding domain fusion with a second fusion of the Gal4 DNA binding domain to the nuclear receptor interaction domain of the coactivator SRC-3 was unaffected by vehicle, CDCA or DPPC, but was stimulated by either DUPC or DLPC (Supp. Fig. 4a). *In vitro*, SRC-3 protein did not bind to GST alone but showed a significant basal interaction with a GST-LRH-1 ligand binding domain fusion protein, as expected[4]. DLPC and DUPC further increased binding of the coactivator by approximately 3 fold, but vehicle, CDCA, or any of a number of other PC species, including DPPC, had little or no effect (Supp. Fig. 4b). DLPC also unexpectedly but specifically decreased binding of an SRC-2 peptide to the LRH-1 ligand binding domain with an IC50 of approximately 500 nM, but DPPC had no effect (Supp. Fig. 4c), and DLPC did not affect rosiglitazone binding to PPARγ (Supp. Fig. 4d).

As a stringent test of specific binding, the purified bacterially expressed hLRH-1 ligand binding domain was incubated with DLPC or DPPC at molar ratios of 1:1 or 1:5 (protein:PC), and the protein was then repurified to eliminate unbound lipids. Specifically bound lipids were extracted and compared to those in a control incubated with buffer alone, or the re-extracted starting DLPC or DPPC by electrospray ionization-mass spectrometry. Phosphatidylethanolamine (PE) and phosphatidylglycerol (PG) species with 16 to 22 carbon acyl chain lengths occupy the ligand binding pocket in the vehicle treated control, with the most abundant peak corresponding to 16:1/18:1 PG (Fig. 1b). DLPC completely replaced these E. coli phospholipids, even at an added lipid to protein molar ratio of only 1:1, but DPPC showed no detectable displacement, even at 1:5 (Fig. 1b). Based on these functional and *in vitro* biochemical results, as well as the extensive structural studies demonstrating phospholipid binding to NR5A receptors[3–5,13,14], we conclude that DLPC and DUPC act *in vitro* as LRH-1 agonists. The functional results indicate that they may also act directly as agonists *in vivo*, although it remains unclear how they might transit the cell membrane and cytosol and enter the nucleus.

PCs are normal dietary nutrients that are efficiently absorbed in the small intestine, and we used the simple route of oral gavage to deliver cholic acid (CA), DLPC, DUPC and DPPC to C5BL/6 mice. These treatments had no apparent toxic effects and did not alter normalized liver weight (Supp. Fig. 5a) or increase serum indicators of liver damage (Supp. Fig. 5b). CA reduced expression of Cyp7A1 and Cyp8B1 and induced SHP, as expected, and DPPC was without significant effect (Fig. 2a). Both DLPC and DUPC significantly induced expression of Cyp7A1, Cyp8B1 and SR-B1, and repressed SHP (Fig. 2a). The substantial induction of Cyp8B1, particularly by DLPC, is in accord with the opposite response in liver specific *Lrh-1* knockouts[1,2], which otherwise show relatively limited alterations in gene expression or liver physiology. The decreased SHP expression is consistent with the induction of the BA biosynthetic enzymes, but was not expected based on the acute response of the isolated SHP promoter in HeLa cells (Supp. Fig. 2a). Since SHP represses its own expression in the liver[8], it is possible that an initial inductive response is followed by an autoregulatory decrease. The induction of Cyp7A1 and Cyp8B1 is lost in liver specific *Lrh-1* knockouts generated by infecting LRH-1 floxed (f/f) mice[2] with adenoviral cre (Ad-Cre) expression vectors (Supp. Fig. 6a, b).

These gene expression changes were associated with a modest but significant increase in the total BA pool and serum BA levels in DLPC and DUPC treated mice (Fig. 2b), consistent with the opposite effect in liver specific *Lrh-1* knockouts[1,2]. These DLPC and DUPC effects were lost in Ad-Cre mediated liver specific knockouts (Supp. Fig. 6c). Both CA and DUPC/DLPC treated mice showed significantly decreased serum free fatty acids (NEFA) (Fig. 2b) and hepatic triglycerides (TG) (Fig. 2c), which was associated with decreased serum glucose in DUPC/DLPC treated, but not CA treated mice (Fig. 2b). Serum and hepatic cholesterol levels were unaffected (Fig. 2b, c). As anticipated based on the effective clearance of phospholipid containing gut derived chylomicrons by the liver, neither DLPC nor DUPC altered expression of SF-1 target genes in the adrenal gland (Supp. Fig. 5c).

Prompted by the lipid and glucose effects in the normal mice, we focused on DLPC, a natural product, and treated insulin resistant leptin receptor deficient *db/db* mice for 2 weeks

by oral gavage, followed by a glucose tolerance test (GTT). An insulin tolerance test (ITT) was carried out after 1 week of additional treatment. Glucose homeostasis was improved in DLPC treated mice, as shown by GTT and ITT (Supp Fig. 7a), as well as lower fasting serum insulin levels (Supp. Fig. 7e). DLPC treatment did not affect body weight or a number of other parameters, but decreased expression of the lipogenic transcription factor SREBP-1c and its downstream targets, and significantly lowered hepatic TG levels in the *db/db* mice (Supp. Fig. 7b–f, Supp. Fig. 8).

To critically test the role of hepatic LRH-1 in these antidiabetic effects, wild type *Lrh-1*$^{f/f}$ and liver specific *Lrh-1*$^{-/-}$ mice (LKO) generated using an Alb-Cre transgene (Supp. Fig. 9a) were fed a high fat diet to induce obesity and insulin resistance (DIO) for 15 weeks. Continuing on the diet, they were treated daily by oral gavage with vehicle or DLPC for 3 weeks, and glucose homeostasis was assessed by GTT and ITT. Loss of LRH-1 did not affect glucose homeostasis in the LKO DIO mice relative to the *Lrh-1*$^{f/f}$ DIO mice (Fig. 3a). As in the *db/db* mice, DLPC treatment substantially improved glucose homeostasis in the *Lrh-1*$^{f/f}$ DIO mice as indicated by GTT and ITT, and these responses were absent in the LKO DIO mice (Fig. 3a). The DLPC treated *Lrh-1*$^{f/f}$ DIO mice also had decreased fasting serum glucose and insulin levels, resulting in an 80% decrease in homeostatic model assessment of insulin resistance (HOMA-IR) (Fig. 3b). Increased insulin sensitivity was confirmed using the hyperinsulinemic-euglycemic clamp, which showed both increased glucose disposal and markedly decreased hepatic glucose production in the DLPC treated mice (Fig. 3c). Increased overall insulin sensitivity was also confirmed by increased insulin dependent phosphorylation of the insulin receptor, IRS-2 and AKT in the DLPC treated *Lrh-1*$^{f/f}$ livers, but not LKO livers (Fig. 3d, Supp. Fig. 9c).

Total body weight and food intake (Supp. Fig. 9b), as well as weights of liver, reproductive fat pads, or brown fat did not differ between the *Lrh-1*$^{f/f}$ and LKO DIO mice. However, the livers of DLPC treated *Lrh-1*$^{f/f}$ DIO mice were less pale and fatty, and decreased lipid deposition was confirmed both histologically and by direct measurement of hepatic TG levels (Fig. 4a, b). NEFA levels were also decreased by DLPC in *Lrh-1*$^{f/f}$, but not LKO DIO livers and serum (Fig. 4b). Hepatic and serum BA levels were significantly increased by DLPC in the *Lrh-1*$^{f/f}$, but not the LKO DIO mice (Fig. 4b). DLPC significantly induced both Cyp7A1 and Cyp8B1 expression in the *Lrh-1*$^{f/f}$ mice, and this specific response was absent in the LKO mice (Supp. Fig. 10a). The expression of additional BA related genes, including the biosynthetic Cyp7B1 and Cyp27A1 and the hepatic BA transporters BSEP and NTCP was not significantly affected by DLPC treatment in *Lrh-1*$^{f/f}$ DIO mice (Supp. Fig. 10a).

In accord with *db/db* results (Supp. Fig. 8), there was little or no effect on hepatic expression of a number of glucose homeostasis and fatty acid oxidation genes (Supp. Fig. 10d, e). However, DLPC markedly decreased expression of genes associated with *de novo* lipogenesis (Fig. 4c), including the lipogenic transcription factor SREBP-1c and its key downstream targets ACC-2, SCD-1 and FASN in *Lrh-1*$^{f/f}$ DIO mice (Fig. 4c). The beneficial effects of DLPC on glucose homeostasis and fatty liver in *Lrh-1*$^{f/f}$ mice fed a high fat diet and infected with a control Ad-GFP vector were also lost in mice in which the *Lrh-1*$^{f/f}$ allele was deleted by Ad-Cre expression (Supp. Fig. 11). Overall, we conclude that LRH-1 is required for the antidiabetic effects of DLPC. However, it remains to be determined whether

its effects are a consequence of being a direct ligand for LRH1, and it remains possible that DLPC activates an alternative signaling cascade or induces biosynthesis of an endogenous LRH-1 ligand.

Here we have identified DLPC as a specific agonist ligand for LRH-1 *in vitro*. Further studies will be needed to address the intriguing questions of whether phospholipid transfer proteins[15] facilitate its transport to the large and dynamic intranuclear pool of phosphatidylcholine[16], and whether DLPC is an endogenous LRH-1 agonist. The ligand responsiveness of LRH-1 is consistent with the identification of synthetic agonists that activate both LRH-1 and SF-1[17]. When expressed in an adrenal cell line, SF-1 is bound by a relatively low molecular weight form of phosphatidic acid with two saturated 14 carbon acyl chains, which acts as an agonist for SF-1 but not LRH-1[18]. Earlier results identified the sphingolipids sphingosine and lyso-sphingomyelin as potential endogenous antagonists of SF-1 transactivation[19]. DLPC does not activate other nuclear receptors, including PPARα or PPARγ, which have previously been reported to be activated by more conventional longer chain phospholipid species[12,20,21]. In the opposite direction, LRH-1 is not activated by conventional PC species, including the C16:0/C18:1 PC reported to specifically bind and activate PPARα in the liver[12]. Phospholipids are emerging as a structurally diverse class of highly specific nuclear receptor ligands.

The beneficial effect of DLPC on steatosis is associated with significantly decreased expression of the transcription factor SREBP-1c and its downstream lipogenic targets. At least 2 complementary mechanisms could contribute to this decrease. Since SREBP-1c autoregulates its own expression[22], the reported functional antagonism of SREBP-1c transactivation by LRH-1[23] could directly inhibit SREBP-1c promoter activity. Since SREBP-1c expression is induced by insulin[24], the DLPC-dependent decrease in serum insulin should also decrease SREBP-1c mRNA. The combination of these two mechanisms could set up a positive regulatory loop in which the initial LRH-1 dependent repression of SREBP-1c expression would decrease steatosis and increase insulin sensitivity, resulting in a decrease in serum insulin. This decrease would then reinforce the decline in SREBP-1c expression and activity, further ameliorating fatty liver and thereby continuing a beneficial cycle (Supp. Fig. 12). This essentially reverses the lipogenic vicious cycle to insulin resistance proposed by McGarry[25], and supported by more recent results with SREBP-1c[26].

These beneficial effects are likely complemented by an increase in fatty acid β-oxidation due to the decrease in acetyl-CoA carboxylase-2 (ACC-2) and its product, malonyl-CoA, which allosterically inhibits CPT-1a enzymatic activity and mitochondrial fatty acid uptake[27]. Decreasing ACC-2 activity in response to either specific anti-sense oligonucleotides[28] or activation of the nuclear receptor CAR[29] increases β-oxidation and has beneficial effects on both steatosis and insulin resistance. Since SCD-1 ablation also protects against hepatic steatosis by decreasing lipogenesis and increasing β-oxidation[30], reduced SCD-1 expression may also increase β-oxidation in response to LRH-1 activation.

We conclude that the identification of DLPC as a useful tool for analysis of LRH-1 function has uncovered an unexpected, LRH-1 dependent PC signaling pathway that can improve fatty acid and glucose homeostasis. These studies suggest DLPC as a promising therapeutic

agent for the treatment of metabolic disorders, and we have initiated a human clinical trial to explore potential beneficial effects in prediabetic patients.

Methods Summary

For transient transfection assays with HeLa, Cos-1 or C3A/HepG2 cells, candidate phospholipids dissolved in ethanol were added to cells for 24h in medium containing 10% charcoal treated FBS. Luciferase expression was assayed and normalized using β-galactosidase expression for transfection efficiency. Transfections were done in triplicate. For binding studies, the hLRH-1 ligand binding domain (LBD), residues 291–541, was expressed as a maltose-binding protein fusion protein, cleaved and purified. It was incubated overnight with or without DLPC and specifically bound lipids were extracted with chloroform/methanol and analyzed using electrospray mass injection-MS in the negative-ion mode to detect and identify phospholipids. LanthaScreen binding studies (Invitrogen) used full length human LRH-1 and PPARγ. For short term animal studies, C57BL/6 mice were orally gavaged with CA, DPPC, DUPC, or DLPC delivered in a standard vehicle every 12h for a total of 5 treatments. Mice were sacrificed 4h after final treatment in the morning of day 3. *Lrh-1* liver specific knockout mice were generated as previously described[2]. For diabetes experiments, *db/db* mice were treated with vehicle or DLPC for 3 weeks. GTT was performed 2 weeks after treatment. After an additional 1 week treatment, ITT was performed. 8–10 week-old male control *Lrh-1*$^{f/f}$ or LKO mice were placed on a high fat diet (45% kcal fat) for 15 weeks. The diet was maintained and mice were treated with vehicle or DLPC by oral gavage. GTT was performed in 18h fasted mice after 2 week treatments. 1 week later, ITT was performed in random fed mice. Hyperinsulinemic clamp (insulin dose = 10 mU/kg/min) was performed in the Diabetes and Endocrinology Research Center at Baylor College of Medicine. All animal experiments were performed according to procedures approved by the Baylor College of Medicine's Institutional Animal Care and Use Committee.

Methods

Materials

Phospholipids were purchased from Avanti Polar Lipids; Fatty acids, cholic acid (CA), and chenodeoxycholic acid (CDCA) from Sigma-Aldrich; Cell culture media and supplements from Invitrogen; Insulin from Eli Lilly and Co.; Human LRH-1 antibody from R&D systems, Antibody against IRβ, IRS2, pSer-Akt, and Akt was from Cell Signaling Technology, Anti-Phosphtyrosine antibody from Millipore; Ad5-CMV-GFP or Cre virus was prepared by the Vector Development Laboratory at the Baylor College of Medicine.

Cell culture and treatments, transient transactivation assays, and siRNA mediated knockdown

HeLa, Cos-1 and C3A/HepG2 cells were cultured in DMEM containing 10% FBS and 1% penicillin/streptomycin antibiotics. 70–80% confluent cells were replated into a 24-well plate with a 1:5 ratio 24h before transfection. Cell culture media were changed 1h before transfection (calcium phosphate method). At 16 hr after transfection, candidate

phospholipids dissolved in ethanol were added to cells for 24h in medium containing 10% charcoal treated FBS. Luciferase expression was assayed and normalized using β-galactosidase expression for transfection efficiency. Transfections were done in triplicate. Plasmids used were pcDNA3 for empty vector (100 ng/well), LRH-1/SF-1 Luc reporter (200 ng/well), actin-β-gal for internal control (150 ng/well), hLRH-1 expression plasmid (100 ng/well), mutant hLRH-1 expression plasmids (100 ng/well, phosphorylation mutant: S238, 243A; sumoylation mutant: K270R; ligand binding mutant: F342W, I426W), Oct4-PP Luc reporter (200 ng/well), and Oct4-PP_{mut} Luc (200 ng/well). Expression plasmids for receptors (100 ng/well) and their cognate luciferase reporters (200 ng/well) used were: $hT_3Rβ$, TK-28T-Luc; hRXRα, TK-CRBPII-Luc; hRARβ, TK-DR5-Luc; mPPARα, mPPARδ, mPPARγ, TK-PPRE×3-Luc; mFXRα, hFXRα, MMTV-TK-ECRE×5-Luc; hLXRα, TK-LXRE×3-Luc; hERα, TK-ERE-Luc; mCAR, hCAR, hPXR, TK-DR4-Luc; mSF-1, mLRH-1, hLRH-1, LRH-1/SF-1 Luc. For mammalian two-hybrid assays, replated HeLa cells in a 24-well plate were transfected with VP-16 (50 ng/well), VP16-hLRH-1 ligand binding domain (50 ng/well), Gal4-SRC-3 RID (100 ng/well), G5-TK-Luc (200 ng/well), and actin-β-gal plasmids (150 ng/well). For siRNA experiments, C3A/HepG2 cells were maintained with MEM containing 10% FBS, 1mM sodium pyruvate, 0.1mM nonessential amino acids, and 1.5 g/L sodium bicarbonate. C3A/HepG2 cells were replated into either a 24-well plate for luciferase assay or a 6-well plate for target gene expression and then transfected with hLRH-1 (Dharmacon, ON-TARGETplus SMARTpool, L-003430-00) or control siRNA pool (Dharmacon, si*CONTROL* non-targeting siRNA pool, D-001206-13-05) using FuGENE 6 (Roche); For the luciferase assay, C3A/HepG2 cells were transfected with LRH-1/SF-1 Luc and actin-β-gal along with siRNA pool. 24h later, ligands were added, and cells were harvested 24h later. To check for knockdown, cell extracts were analyzed by immunoblot using an antibody against hLRH-1.

In vitro binding assays

GST pulldown was used to examine the interaction between hLRH-1 ligand binding domain and SRC-3 *in vitro* as described[4]. GST alone and GST hLRH-1 ligand binding domain (amino acid residues, 185–541) were expressed in DH5α strain *E. coli* with 0.5mM IPTG for 4h and then purified with glutathione-sepharose beads (GE Healthcare). GST proteins were incubated overnight at 4°C in 50mM Tris-HCL (pH 7.6), 0.2% Tween-20, 100 mg/ml BSA, and 300mM NaCl with various phospholipids. Full-length [^{35}S]methionine-labeled SRC-3 proteins (2 μL) were added to each reaction and incubated for 2h at 4°C. Unbound and nonspecific proteins were removed by washing five times with the same buffer. Specifically bound proteins were eluted by treatment with SDS sample buffer, subjected to SDS- PAGE, and visualized by autoradiography. The amount of specifically bound SRC-3 proteins was determined by densitometry (Personal Densitometer SI, Molecular Dynamics).

Lanthascreen assays were as described by the manufacturer (Invitrogen) using full length human LRH-1 and a fluorescein tagged SRC-2 coactivator peptide, and PPARγ and Fluoromone[31].

For mass spectrometry, the hLRH-1 ligand binding domain (LBD), residues 291–541, was expressed as a maltose-binding protein fusion protein, cleaved and purified as described

previously[4]. The pure protein was stored in a final buffer containing 150mM NaCl, 20mM HEPES and 5% glycerol. For binding studies, DLPC or DPPC dissolved in ethanol was evaporated in a clean glass cuvette at 50° C under a stream nitrogen gas. 2 mL of buffer containing 150mM NaCl, 20mM HEPES (pH=7.5) and 5% glycerol was added to the cuvette containing dried DLPC or DPPC and was sonicated until the solution was optically clear. hLRH-1 LBD was then added to the DLPC or DPPC vesicles at a ratio of 1:1 or 1:5 (hLRH-1 LBD:PC). The mixture was incubated for one hour at 37° C followed by 24 hrs at 11°C. The hLRH-1 – lipid complex was then purified by size exclusion chromatography to remove unbound phospholipids. Protein purity was assed by SDS-PAGE. Bound lipids were analyzed using electrospray mass injection-MS in the negative-ion mode to detect and identify phospholipids. Approximately 6 mg of hLRH-1 LBD or the hLRH-1 LBD:lipid complexes was extracted with a 2:1 chloroform/methanol solution, diluted in 200 mL chloromethylene and analyzed by negative-ion ESI-MS on a Thermo LTQ FTMS using direct injection analysis with electrospray ionization. The high-resolution analyses were performed in the FTMS at a resolution of 100000 at 400 m/z. The MS/MS experiments were done in the ion trap portion of the instrument with a mass selection of 3 amu and a normalized collision energy of 30 V. The major phospholipid species were identified by accurate mass measurements and MS/MS via collisionally induced dissociation (CID), which yields product ions characteristic of the head groups and attached fatty acids.

Animal studies

C57BL/6 mice and *db/db* mice were purchased from Harlan laboratories, Inc. 8-week-old male C57BL/6 mice were orally gavaged with CA, DPPC, DUPC, or DLPC at a dose of 100 mg/kg body weight, delivered in a standard vehicle for delivery of hydrophobic compounds (4:1 of PEG-400 and Tween-80) every 12h for a total of 5 treatments. Mice were sacrificed 4h after final treatment in the morning of day 3. Harvested tissues were immediately frozen in liquid nitrogen for molecular studies. 12-week old male *db/db* mice were used for diabetes studies. *db/db* mice were given compounds (vehichle or DLPC, n=5 animals/group) at the dose of 100 mg/kg/day for 3 weeks. GTT (1.5 g/kg intraperitoneal injection) was performed in 18 hr fasted mice after 2 week treatments. 1 week later, ITT (2 U/kg intraperitoneal injection) was performed in *ad libitum* fed mice. Serum insulin levels were determined using Rat/Mouse Insulin ELISA Kit from Linco Research, Inc. *Lrh-1*$^{f/f}$ mice[2] were maintained on mixed C57BL6/129 backgrounds were generously given by the Kliewer/Mangelsdorf laboratory. In brief, 4-month-old male *Lrh-1*$^{f/f}$ littermates were tail vein injected with either Ad5-CMV-GFP (3×10^9 pfu) or Ad5-CMV-Cre (3×10^9 pfu). For acute experiments, these mice were orally gavaged daily with each compound starting 2 weeks after adenovirus injection as described in C57BL/6 mice above. Liver specific *Lrh-1* ablation (LKO) was also achieved by crossing *Lrh-1*$^{f/f}$ mice with albumin-Cre transgenic mice obtained from the O'Malley laboratory at BCM. To confirm tissue-specific deletion of exon 5 of *Lrh-1*, genomic DNA was extracted from tail, liver, and intestine, and PCR analysis was performed as shown previously[2]. For diabetes experiments, 8–10 week-old male control *Lrh-1*$^{f/f}$ or LKO mice were placed on a high fat diet (HFD, Research diets; 45% kcal fat) for 15 weeks. The diet was maintained and mice were treated with vehicle or DLPC (dose of 100 mg/kg/day) by oral gavage. GTT (2 g/kg intraperitoneal injection) was performed in 18h fasted mice after 2 week treatments. 1 week later, ITT (1 U/kg,

intraperitoneal injection) was performed in random fed mice. Glucose levels were analyzed using a glucometer (LifeScan Inc.). Insulin resistance (homeostasis model assessment-insulin resistance, HOMA-IR) was calculated as following: fasting glucose (mg/dL) × fasting insulin (μU/mL)/405. Hyperinsulinemic clamp (insulin dose is 10 mU/kg/min) was performed and calculated as described in our previous publication[32]. 15 weeks HFD fed either Ad-GFP or Ad-Cre infected *Lrh-1*$^{f/f}$ mice were used for diabetes study as shown above. Mice were housed in a temperature-controlled room in pathogen-free facilities on 12h light/dark cycle (07:00 on, 19:00 off) and had free access to water and standard chow diet. All animals received humane care according to the criteria outlined in the "Guide for the Care and Use of Laboratory Animals" prepared by the National Academy of Sciences and published by the National Institutes of Health.

RNA isolation and mRNA quantification

Total RNA was isolated from C3A/HepG2 cells or snap-frozen liver tissues using Trizol Reagent (Invitrogen) and prepared for the cDNA with QuantiTect reverse transcriptase (Qiagen). Hepatic gene expression (n=4–5) was determined by qPCR using FastStart SYBR Green master (ROX) (Roche). mRNA levels were normalized by the 36B4 gene. Primer information can be provided upon request.

Serum and tissue lipid analysis

Blood was collected from the orbital plexus and transferred into gel/clot activator tubes (Terumo). Samples were centrifuged at 6,000g for 5min to separate serum. To extract bile acids from liver or intestine, each tissue was weighed and homogenized in 75% ethanol. The homogenate was incubated at 50°C for 2h to extract bile acids and centrifuged at 6,000g for 10min at 4°C. The bile acid content of the supernatant was determined and normalized with tissue weight used. To extract other lipids, snap-frozen liver fragments were weighed and homogenized in 9 volume of PBS. 200 μL of the homogenate was transferred into 1200 μL of chloroform: methanol (2:1; v/v) mixture and mixed vigorously for 30sec. 100 μL of PBS was then added, and the resulting suspension was mixed vigorously for 15sec then centrifuged at 3,000 rpm for 10min at 4°C. 200 μL of the chloroform: methanol layer (bottom phase) was transferred into tube and evaporated for dryness. The dried lipid residue was resuspended in 100 μL of 1% Triton X100 in absolute ethanol for 4hr with constant rotation. Bile acids levels were measured using the bile acid L3K assay kit (Diagnostic Chemicals). Cholesterol and triglyceride levels were determined by assay kits from Thermo DMA Inc. Free fatty acids were assayed using a kit obtained from WAKO Chemicals Inc.

In vivo insulin stimulation and analysis of insulin signaling

Mice were fasted overnight and injected intraperitoneally with insulin (1 U/kg) or PBS. 5min after injection, tissues were removed, frozen in liquid nitrogen, and stored at −80°C until use. For protein extraction, tissues were homogenized in a cold lysis buffer (50mM Tris-HCl, pH7.4; 1% NP-40; 0.5% sodium deoxycholate; 150mM NaCl; 1mM EDTA) containing protease and phosphatase inhibitor cocktails (Roche). After homogenization, the tissue lysates were allowed to solubilize for 1h at 4°C with rotation, and then were

centrifuged at 14,000 rpm for 30min at 4°C. The supernatants were used for immunoprecipitations and immunoblot analyses of insulin signaling proteins.

Histology

Liver was removed and pieces were fixed in 10% (v/v) neutralized formalin solution (J.T. Baker), embedded in paraffin, sectioned at 5μm, and stained with hematoxylin and eosin (H & E). For Oil Red O staining, frozen liver tissues embedded in O.C.T compound (Tissue-Tek) were used. Histologic analysis performed in the Comparative Pathology Laboratory at Baylor College of Medicine.

Supplementary Material

Refer to Web version on PubMed Central for supplementary material.

Acknowledgments

We thank Steven A. Kliewer and David J. Mangelsdorf (UT Southwestern Medical Center) for the generous gift of *Lrh-1*$^{f/f}$ mice, Austin J. Cooney for the Oct4 promoter constructs, Charity Mills and Dana Kuruvilla for experimental assistance, the BCM Diabetes Endocrine Research Center (supported by NIH DK-079638) and the services of the Mouse Metabolism Core for hyperinsulinemic clamp studies, and the current and previous members of the Moore laboratory for helpful discussions and technical support. Supported by NIH R01 DK068804, the Alkek Foundation and the Robert R. P. Doherty Jr. Welch Chair in Science to D.D.M., and NIH R01 CA134873 to P.R.G.

References

1. Mataki C, et al. Compromised intestinal lipid absorption in mice with a liver-specific deficiency of the Liver Receptor Homolog 1. Mol Cell Biol. 2007
2. Lee YK, et al. Liver Receptor Homolog-1 Regulates Bile Acid Homeostasis But Is Not Essential for Feedback Regulation of Bile Acid Synthesis. Mol Endocrinol. 2008
3. Krylova IN, et al. Structural analyses reveal phosphatidyl inositols as ligands for the NR5 orphan receptors SF-1 and LRH-1. Cell. 2005; 120:343–355. [PubMed: 15707893]
4. Ortlund EA, et al. Modulation of human nuclear receptor LRH-1 activity by phospholipids and SHP. Nat Struct Mol Biol. 2005; 12:357–363. [PubMed: 15723037]
5. Wang W, et al. The crystal structures of human steroidogenic factor-1 and liver receptor homologue-1. Proc Natl Acad Sci U S A. 2005; 102:7505–7510. [PubMed: 15897460]
6. Cusi K. Nonalcoholic fatty liver disease in type 2 diabetes mellitus. Curr Opin Endocrinol Diabetes Obes. 2009; 16:141–149. [PubMed: 19262374]
7. Watanabe M, et al. Bile acids lower triglyceride levels via a pathway involving FXR, SHP, and SREBP-1c. J Clin Invest. 2004; 113:1408–1418. [PubMed: 15146238]
8. Lee YK, Parker KL, Choi HS, Moore DD. Activation of the Promoter of the Orphan Receptor SHP by Orphan Receptors That Bind DNA as Monomers. J Biol Chem. 1999; 274:20869–20873. [PubMed: 10409629]
9. Gu P, et al. Orphan nuclear receptor LRH-1 is required to maintain Oct4 expression at the epiblast stage of embryonic development. Mol Cell Biol. 2005; 25:3492–3505. [PubMed: 15831456]
10. Lee YK, Choi YH, Chua S, Park YJ, Moore DD. Phosphorylation of the hinge domain of the nuclear hormone receptor LRH-1 stimulates transactivation. J Biol Chem. 2006; 281:7850–7855. [PubMed: 16439367]
11. Chalkiadaki A, Talianidis I. SUMO-dependent compartmentalization in promyelocytic leukemia protein nuclear bodies prevents the access of LRH-1 to chromatin. Mol Cell Biol. 2005; 25:5095–5105. [PubMed: 15923626]

12. Chakravarthy MF, et al. Identification of a Physiologically Relevant Endogenous Ligand for PPARalpha in Liver. Cell. 2009; 138:476–488. [PubMed: 19646743]
13. Li Y, et al. Crystallographic identification and functional characterization of phospholipids as ligands for the orphan nuclear receptor steroidogenic factor-1. Mol Cell. 2005; 17:491–502. [PubMed: 15721253]
14. Sablin EP, et al. Structure of SF-1 bound by different phospholipids: evidence for regulatory ligands. Mol Endocrinol. 2009; 23:25–34. [PubMed: 18988706]
15. Kang HW, Wei J, Cohen DE. PC-TP/StARD2: Of membranes and metabolism. Trends Endocrinol Metab. 2010; 21:449–456. S1043-2760(10)00036-6 [pii]. 10.1016/j.tem.2010.02.001 [PubMed: 20338778]
16. Hunt AN. Dynamic lipidomics of the nucleus. J Cell Biochem. 2006; 97:244–251. [PubMed: 16240373]
17. Whitby RJ, et al. Identification of small molecule agonists of the orphan nuclear receptors liver receptor homolog-1 and steroidogenic factor-1. J Med Chem. 2006; 49:6652–6655. [PubMed: 17154495]
18. Li D, et al. cAMP-Stimulated Interaction Between Steroidogenic Factor-1 and Diacylglycerol Kinase-{theta} Facilitates Induction of CYP17. Mol Cell Biol. 2007
19. Urs AN, Dammer E, Sewer MB. Sphingosine regulates the transcription of CYP17 by binding to steroidogenic factor-1. Endocrinology. 2006; 147:5249–5258. [PubMed: 16887917]
20. Lee H, et al. Role for peroxisome proliferator-activated receptor alpha in oxidized phospholipid-induced synthesis of monocyte chemotactic protein-1 and interleukin-8 by endothelial cells. Circ Res. 2000; 87:516–521. [PubMed: 10988245]
21. McIntyre TM, et al. Identification of an intracellular receptor for lysophosphatidic acid (LPA): LPA is a transcellular PPARgamma agonist. Proc Natl Acad Sci U S A. 2003; 100:131–136. [PubMed: 12502787]
22. Amemiya-Kudo M, et al. Promoter analysis of the mouse sterol regulatory element-binding protein-1c gene. J Biol Chem. 2000; 275:31078–31085. [PubMed: 10918064]
23. Kanayama T, et al. Interaction between sterol regulatory element-binding proteins and liver receptor homolog-1 reciprocally suppresses their transcriptional activities. J Biol Chem. 2007; 282:10290–10298. [PubMed: 17283069]
24. Shimomura I, et al. Insulin selectively increases SREBP-1c mRNA in the livers of rats with streptozotocin-induced diabetes. Proc Natl Acad Sci U S A. 1999; 96:13656–13661. [PubMed: 10570128]
25. McGarry JD. What if Minkowski had been ageusic? An alternative angle on diabetes. Science. 1992; 258:766–770. [PubMed: 1439783]
26. Li S, Brown MS, Goldstein JL. Bifurcation of insulin signaling pathway in rat liver: mTORC1 required for stimulation of lipogenesis, but not inhibition of gluconeogenesis. Proc Natl Acad Sci U S A. 2010; 107:3441–3446. 0914798107 [pii]. 10.1073/pnas.0914798107 [PubMed: 20133650]
27. Kim KH. Regulation of mammalian acetyl-coenzyme A carboxylase. Annu Rev Nutr. 1997; 17:77–99. [PubMed: 9240920]
28. Savage DB, et al. Reversal of diet-induced hepatic steatosis and hepatic insulin resistance by antisense oligonucleotide inhibitors of acetyl-CoA carboxylases 1 and 2. J Clin Invest. 2006; 116:817–824. [PubMed: 16485039]
29. Dong B, et al. Activation of nuclear receptor CAR ameliorates diabetes and fatty liver disease. Proc Natl Acad Sci U S A. 2009; 106:18831–18836. 0909731106 [pii]. 10.1073/pnas.0909731106 [PubMed: 19850873]
30. Dobrzyn P, et al. Stearoyl-CoA desaturase 1 deficiency increases fatty acid oxidation by activating AMP-activated protein kinase in liver. Proc Natl Acad Sci U S A. 2004; 101:6409–6414. [PubMed: 15096593]
31. Vidovic D, Busby SA, Griffin PR, Schurer SC. A combined ligand- and structure-based virtual screening protocol identifies submicromolar PPARgamma partial agonists. Chem Med Chem. 2011; 6:94–103.10.1002/cmdc.201000428 [PubMed: 21162086]
32. Ma K, Saha PK, Chan L, Moore DD. Farnesoid X receptor is essential for normal glucose homeostasis. J Clin Invest. 2006; 116:1102–1109. [PubMed: 16557297]

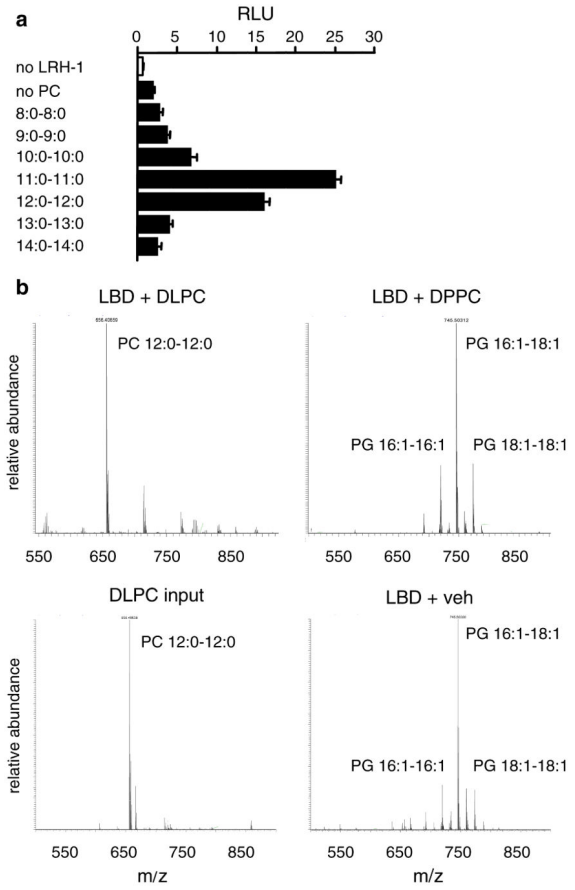

Figure 1. DLPC activates and binds hLRH-1

a, , HeLa cells were transfected with a hLRH-1 expression vector and a luciferase reporter and treated with 100 μM of indicated PCs. Error bars represent mean ± s.e.m. **b.** The hLRH-1 ligand binding domain (LBD) was expressed and purified as described previously[5] and was incubated at molar ratios of 1:1 and 1:5 (hLRH-1 LBD:PC) with DLPC, DPPC or vehicle for two hours at 37°C, and then repurified by size exclusion chromatography to remove unbound phospholipids. Bound lipids were analyzed using electrospray mass injection-MS in the negative-ion mode. Results with DLPC (1:1), DPPC (1:5) and vehicle are shown, along with analysis of re-extracted DLPC; DLPC (1:5) and DPPC (1:1) incubations were very similar to those shown. The re-extracted DPPC peak is at 768.5, and is not detectable in any of the DPPC incubations.

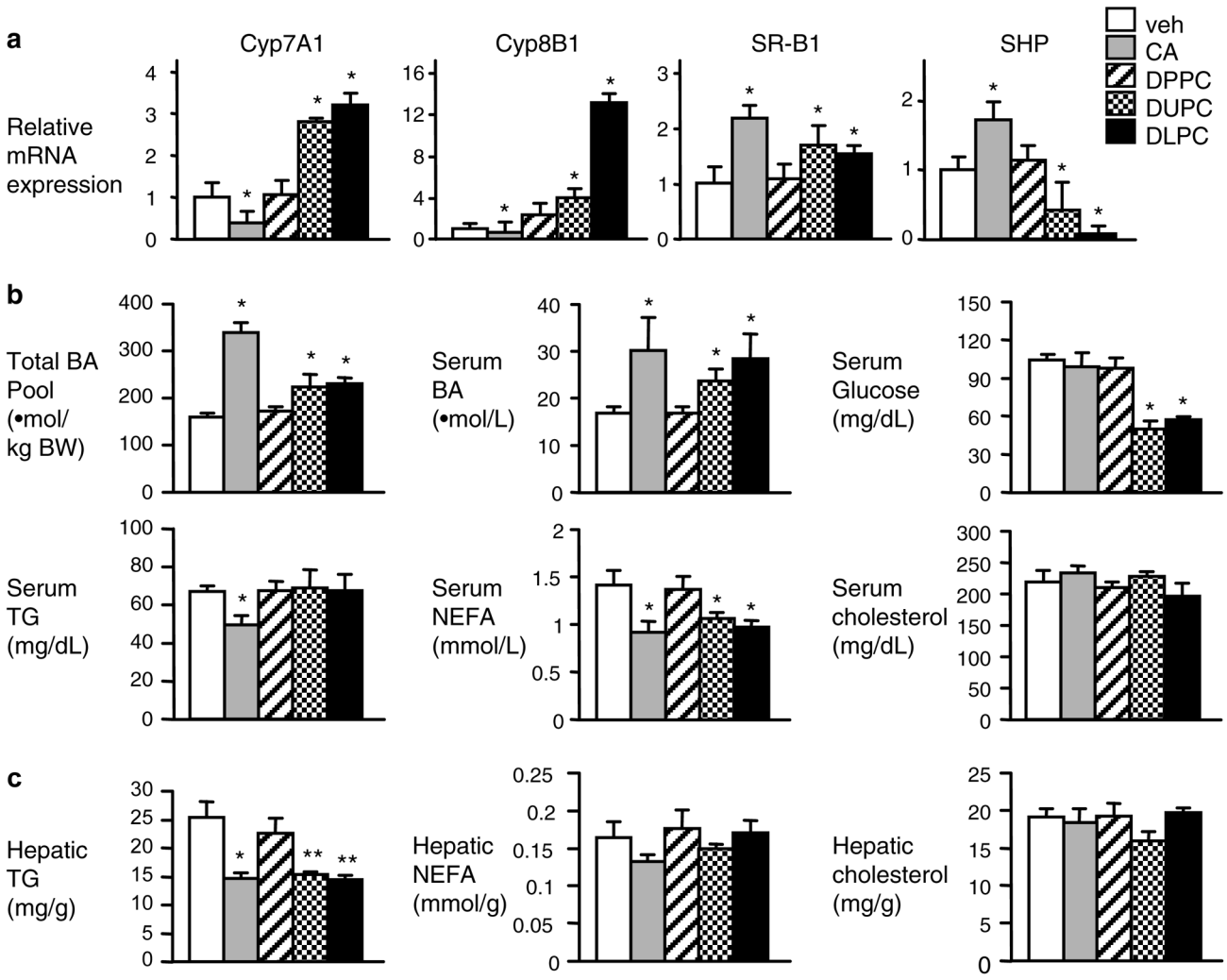

Figure 2. DLPC and DUPC modulate expression of LRH-1 target genes in liver

a, , 8-week-old male C57BL/6 mice were challenged orally with vehicle, CA, DPPC, DUPC, and DLPC for 3 days. Total liver RNA was isolated and prepared for the cDNA. Hepatic gene expression was determined using qPCR. mRNA levels are relative to 36B4. **b**, Total BA pool and serum BAs, glucose, TG, NEFA, and cholesterol were measured in the same animals. **c**, Hepatic TG, NEFA, and cholesterol were measured in the same animals. Error bars represent mean ± s.e.m. (*P<0.05, **P<0.01 vs veh; n=5 animals/group).

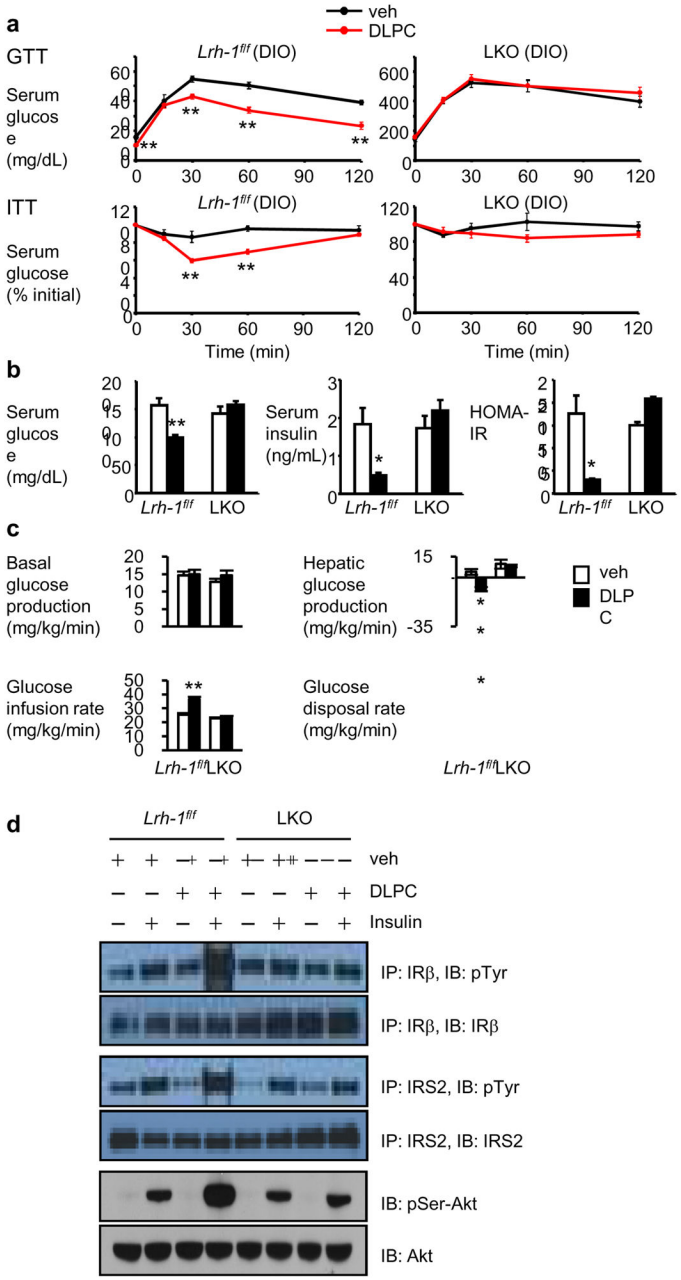

Figure 3. DLPC improves glucose homeostasis in mouse models of insulin resistance

a, , Glucose and insulin tolerance were assessed in *Lrh-1*$^{f/f}$ and LKO DIO mice 2–3 weeks after vehicle or DLPC treatment. **b**, Fasting serum glucose and insulin levels were measured in the same animals shown in **a**. HOMA-IR was calculated from fasting serum glucose and insulin levels. **c,** The high dose (10 mU/kg/min) hyperinsulinemic-euglycemic clamp (insulin dose (10 mU/kg/min) was used to assess glucose homeostasis in *Lrh-1*$^{f/f}$ DIO mice following 3 weeks of vehicle or DLPC treatment. **d**, Hepatic insulin signaling was examined in *Lrh-1*$^{f/f}$ and LKO DIO mice 2 weeks after vehicle or DLPC treatment. Liver tissue homogenates from 3 mice per group were pooled and immunoprecipitation and

immunoblotting was as indicated. Results are representative of 3 independent experiments. Error bars represent mean ± s.e.m. (*P<0.05, **P<0.01 vs *Lrh-1*$^{f/f}$ DIO mice treated with veh; n=4 animals/group).

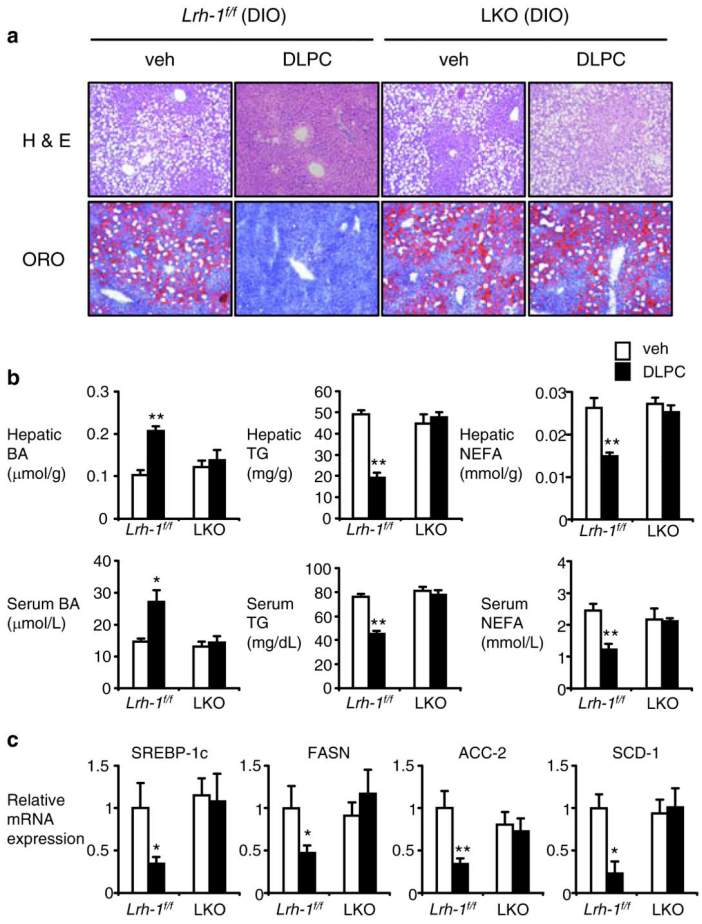

Figure 4. DLPC reduces liver fat accumulation by suppressing lipogenesis

a, , Liver sections from *Lrh-1*$^{f/f}$ and LKO DIO mice treated for 3 weeks with vehicle or DLPC were stained with Hematoxylin/Eosin (H & E) for general morphology or Oil Red O (ORO) for lipid accumulation. Original magnification, X10. **b**, Hepatic and serum BA, TG, and NEFA levels were measured in the same mice described in **a. c**, Lipogenic gene expression in the liver was determined using qPCR. mRNA levels are relative to 36B4. Error bars represent mean ± s.e.m. (*P<0.05, **P<0.01 vs *Lrh-1*$^{f/f}$ DIO mice treated with veh; n=4 animals/group).